Hydrogen Storage

DOI: 10.1002/ange.201403610

A Metal-Free Strategy to Release Chemisorbed H_2 from Hydrogenated Boron Nitride Nanotubes**

*Lisa Roy, Sourav Bhunya, and Ankan Paul**

Abstract: *Chemisorbed hydrogen on boron nitride nanotubes (BNNT) can only be released thermally at very high temperatures above 350 °C. However, no catalyst has been identified that could liberate H_2 from hydrogenated BN nanotubes under moderate conditions. Using different density functional methods we predict that the desorption of chemisorbed hydrogen from hydrogenated BN nanotubes can be facilitated catalytically by triflic acid at low free-energy activation barriers and appreciable rates under metal free conditions and mildly elevated temperatures (40–50 °C). Our proposed mechanism shows that the acid is regenerated in the process and can further facilitate similar catalytic release of H_2, thus suggesting all the chemisorbed hydrogen on the surface of the hydrogenated nanotube can be released in the form of H_2. These findings essentially raise hope for the development of a sustainable chemical hydrogen storage strategy in BN nanomaterials.*

In the ardent search toward the realization of a hydrogen-based energy infrastructure, the most formidable challenge lies in its safe and efficient storage.[1] Materials with a facile hydrogenation and dehydrogenation pattern along with easy transportation possibilities are deemed as feasible alternatives to hydrocarbon fuels.[2] Due to the high gravimetric content and fast catalytic release of H_2, ammonia borane (AB) (19.6 wt % H_2) is the cornerstone of chemical hydrogen storage.[3] However, the regeneration of AB from the spent fuel by the newly devised technique constituting of the rehydrogenation by hydrazine[4] may not be sustainable on the long run, because hydrazine is obtained from ammonia, which itself is derived from the energy-intensive Haber–Bosch industrial process.[5] Other allied BN materials like BN nanotubes and fullerenes have been under scrutiny as potential hydrogen storage materials.[6–10] Ma and co-workers demonstrated that multiwalled BN nanotubes can adsorb up to 2.6 wt % of H_2 under room temperature and 10 MPa pressure.[6] Tang et al. found about 4.2 wt % of hydrogen adsorption in collapsed BNNTs at similar conditions.[7] Additionally, theoretical studies opine that up to 50 % of the exterior surface of single-walled BNNTs could be covered with chemisorbed hydrogens, which accounts for greater than 4 wt % of H_2 storage.[11] It was further shown that most of the H_2 adsorbed in the BN nanotubes is in the chemisorbed form,[12] which could be released above 350 °C.[6,7] In structural and electronic analogues of BNNTs like single-walled carbon nanotubes and graphene, several groups have achieved chemisorption of H_2 by exposing the carbon-based materials to a stream of atomic hydrogen and by Birch reduction.[13,14] Although 70 % of the nanotubes was hydrogenated, those hydrogens are thermally released only above 600 °C.[13a] Unfortunately, the high-temperature release of the chemisorbed H_2 is a big impediment in the realization of a sustainable hydrogen storage strategy through chemisorption of H_2 in BN and carbon nanotubes. Hence, the design of a catalyst that could effectively dislodge H_2 from chemisorbed hydrogenated nanotubes under ambient conditions and preferably at a temperature not higher than the operational temperature of hydrogen fuel cells (80 °C), would certainly be a step toward realizing sustainable hydrogen storage in BN nanomaterials.

In a recent study we have shown that the hydrogen atoms in hydrogenated BNNTs mimic those of ammonia borane and react in a similar chemical fashion to certain bifunctional reagents.[15] Our earlier report revealed that hydrogens on HBNNTs display dual behavior, with a hydridic character for H on -B–H moieties and a protic character for H on -N–H moieties, which is characteristic of amine boranes in general.[15] We showed that this peerless attribute can be used to hydrogenate aldehydes, *N*-heterocyclic carbenes, and other similar substrates through concerted proton and hydride transfer,[15] which were also observed for ammonia borane.[16] We propose that this property of the chemisorbed hydrogens can be further exploited to release H_2 under ambient conditions at appreciable rates through proper catalyst design. In recent years several catalysts have been developed to release H_2 from ammonia borane.[17] Our preliminary efforts revealed that the popular transition metal catalysts used for ammonia borane dehydrogenation would fail to release H_2 from hydrogenated BN nanotubes due to expected issues of steric encumbrance in accessing the chemisorbed hydrogens on the nanotube surface by the catalytic center.[18] We envisaged that smaller molecules having a relatively simpler structure and known to effectuate the release of H_2 from ammonia borane could easily access the B–H and N–H hydrogens of hydrogenated BN nanotubes. Strong Lewis and Brønsted acids have been reported to catalyze the dehydrocoupling of amine boranes.[19] Baker et al. were the first to propose a "metal-free" initiation of stoichiometric H_2 loss from AB with the aid of Brønsted acids like triflic acid ($HOSO_2CF_3$) in diglyme under mild conditions ($\approx$60 °C).[19b]

[*] L. Roy, S. Bhunya, Dr. A. Paul
Raman Centre for Atomic Molecular and Optical Sciences
Indian Association for the Cultivation of Science
2A & 2B, Raja S.C. Mullick Road, Kolkata, 700032 (India)
E-mail: rcap@iacs.res.in

[**] A.P. thanks the DST FASTRACK (NO-SR/FT/CS-118/2011) for providing research funds. L.R. and S.B. acknowledge research fellowships of the CSIR (India).

Supporting information for this article is available on the WWW under http://dx.doi.org/10.1002/anie.201403610.

In a recent theoretical study we have unravelled the mechanism of this dehydrogenation process.[20] Based on the insights derived from this study we propose that triflic acid (TfOH) would act as an efficient dehydrogenation catalyst for hydrogenated BN compounds in nonproton acceptor or non-nucleophilic solvents.[18] Herein, through computational studies we show that TfOH can facilitate the H_2 desorption from hydrogenated BN nanotubes in gas-phase or non-ether solvents. We have used 50% hydrogenated zigzag BNNT with hydrogenated terminals of (8,0) chirality of approximate lengths around 1 nm and 2 nm (henceforth referred to as 1-HBNNT and 2-HBNNT, respectively) as computational models. Scheme 1 illustrates the details of our proposed mechanism of hydrogen desorption from a hydrogenated BNNT aided by TfOH.

All molecular geometries of the intermediates and transition states investigated in this work have been optimized in the Gaussian09 suite of programs at the B3LYP/B1 level in vacuum, B1 designating basis-set combination of Pople's 6-31++G(d,p) family of basis on the reaction center along with STO-3G on the rest of the system.[18] Crucial transition states and intermediates were further optimized in the gas phase at B3LYP/B1′, where B1′ basis set constitutes of 6-31++G(d,p) basis on the reaction center and 6-31G(d) on the rest of the system. The nature of the stationary points was characterized by harmonic vibrational frequencies computed at the same level of theory with intermediates having all real frequencies and transition states having a single imaginary frequency. The intrinsic reaction coordinate (IRC) technique was applied, when necessary, to verify that the transition states are connected by the right intermediates. Single-point gas-phase and solvent-phase (in acetonitrile solvent, $\varepsilon = 35.68$) computations were carried out on the B3LYP[21a] optimized geometries with ωB97XD,[21b] M05-2X,[21c] and M06-2X[21d] functional employing 6-31++G(d,p) basis functions on all the atoms (B2 basis set combination). To compensate for the damping of translational and rotational degrees of freedom in the solvent phase, Gibbs free energies (denoted by the SPC suffix) were computed using solvent-phase entropies, which in turn were derived by scaling gas-phase entropies by an empirical factor of 0.5, which is a standard practice.[22] The CPCM[23] technique has been chosen, because continuum solvent models are reported to give satisfactory results at the solid–liquid interface.[24] Additional details are provided in the Supporting Information (SI). The text discussed henceforth refers to the thermokinetics predicted by ωB97XD.

We investigated the dehydrogenation of chemisorbed hydrogens at the middle of a BN nanotube, because we consider our model nanotube to be a smaller piece of a larger nanotube and as it would minimize finite size effects in our computation. The coordination of one TfOH to 1-HBNNT is an energetically favorable process, with $\Delta E(s) = -11.1$ kcal mol^{-1} with respect to the separated reactants. This leads to the formation of an intermediate **1**, which shows dipole–dipole attractive electrostatic interaction between the hydride (of B–H) of 1-HBNNT and the proton of TfOH. We observe a similar minimum for the 2 nm long analogue (**1′**), with a comparable geometry and stabilization gain. Unlike water

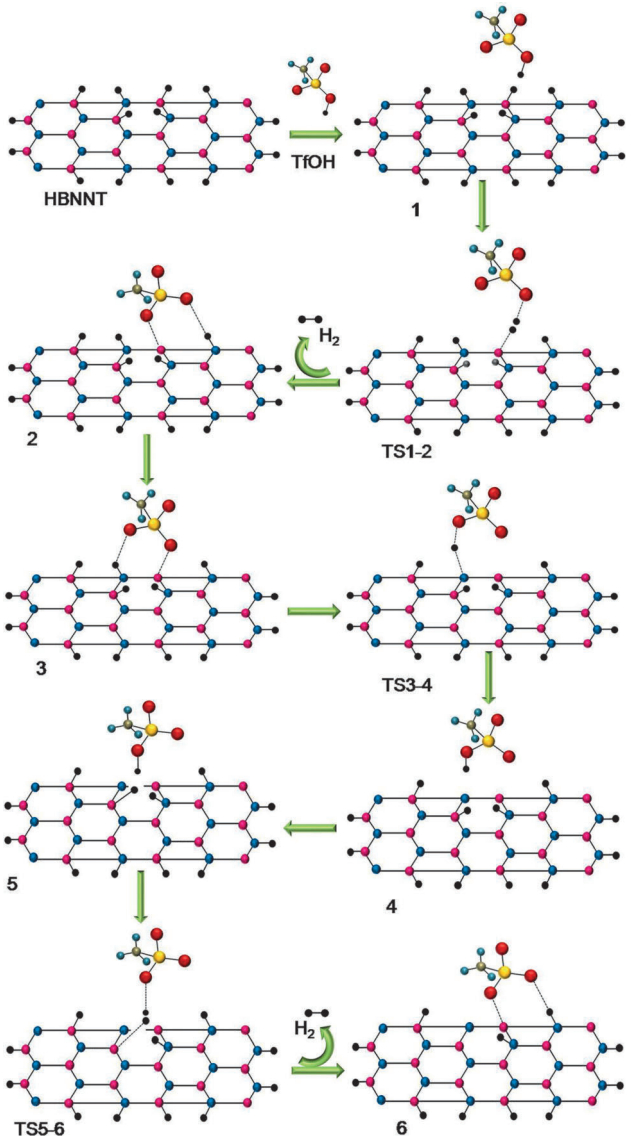

Scheme 1. Proposed mechanistic pathway of catalytic dehydrogenation of chemisorbed hydrogens on a boron nitride nanotube initiated by triflic acid. Color codes for atoms: B (pink), N (blue), O (red), S (yellow), H (black), C (tan), and F (aqua).

or ether solvents, the protonation of CH_3CN by the -SO_3H group is not observed by IR spectrum.[25] Furthermore, the OH stretching frequency of -SO_3H groups at around 3000 cm^{-1} is in agreement with hydrogen-bonded dimeric species of the acid.[25] Triflic acid is likely to exist as dimer in acetonitrile. The free energy cost for dissociation of the triflic acid dimer $(TfOH)_2$ is estimated to be 5.1 kcal mol^{-1}, whereas the stabilization gained in the formation of intermediate **1** from one TfOH and one 1-HBNNT is −4.7 kcal mol^{-1}. This suggests that the binding of two monomers to two separated HBNNTs should result in a stabilization gain of free energy by −9.4 kcal mol^{-1}. So the overall reaction as shown in Scheme 2 should proceed by splitting the triflic acid dimer into monomeric units and the association of the monomers with two separated hydrogenated BN nanotubes. Then the

$[(TfOH)_2] \longrightarrow 2 \times [TfOH]$ $\Delta G(s)_{SPC} = 5.1$

$2 \times [TfOH] + 2 \times [HBNNT] \longrightarrow 2 \times [1]$ $\Delta G(s)_{SPC} = 2 \times -4.7 = -9.4$

$[(TfOH)_2] + 2 \times [HBNNT] \longrightarrow 2 \times [1]$ $\Delta G(s)_{SPC} = -4.3$

Scheme 2. Equations showing the formation of intermediate **1** from the splitting of the acid dimer in the presence of the hydrogenated BN nanotube. The solvent-phase-corrected free energy values are given in kcal mol^{-1}.

whole transformation would involve a $\Delta G(s)_{SPC} = -4.3$ kcal mol^{-1}. This predicts that in the equilibrium, intermediate **1** would be the predominating species before the dehydrogenation initiates.

The reaction ensues through the transfer of a triflic acid proton (**H**-OSO_2CF_3) to the hydride of the B–H moiety of HBNNT leading to the formation of molecular H_2 and a triflate anion. However, in our earlier computational analysis we have found that for ammonia borane such a reaction is triggered by a boronium cation initiator solvated in an ether cage; this finding was further supported by dynamical calculations.[20] Moreover, our present theoretical calculations predict concomitant formation and release of H_2 from the HBNNT surface (Scheme 1), which is different to its chemical analogue AB, in which H_2 is held by the boronium cation species before it is released into the surrounding.[20] The transition states involving the protonolysis of B–H hydride by the O–H proton, which initiates the formation of one H_2 molecule, are very similar in geometry to both, 1-HBNNT and 2-HBNNT, suggesting the reliability of our computational models and the methods used. The H–H distances of 0.90 and 0.95 Å and the B–H distance of around 1.4 Å for the corresponding transition states of 1-HBNNT and 2-HBNNT, respectively, are also reflective of a concomitant formation and release of H_2 (Figure 1). The gas-phase zero-point-corrected total energy barrier, $\Delta E^{\ddagger}(g)$ and Gibbs free energy barrier, $\Delta G^{\ddagger}(g)$ for H_2 release from 1-HBNNT (**TS1-2**) is predicted to be 10.2 and 11.7 kcal mol^{-1}, respectively. The corresponding energy of activation for the removal of one H_2

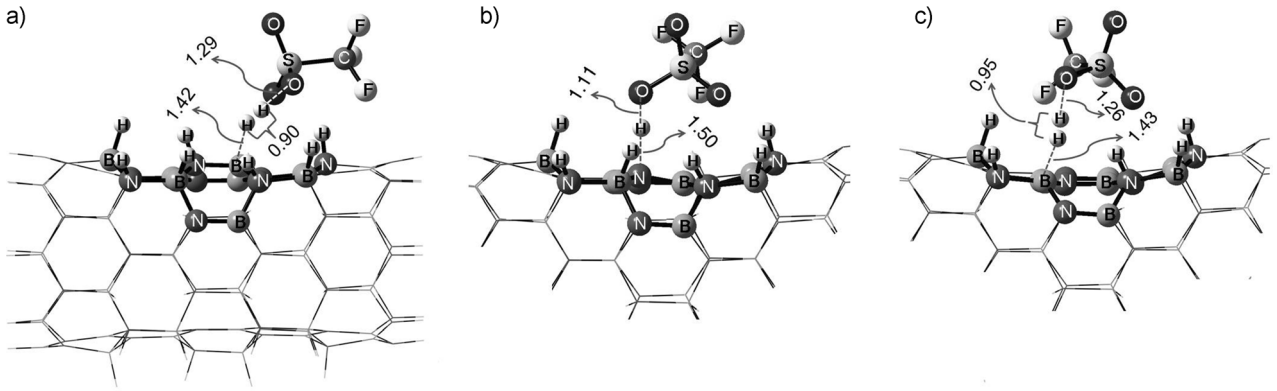

Figure 1. a) Optimized geometry of TS1-2. Partial view of the optimized geometry of b) TS3-4 and c) TS5-6. (Full optimized geometries are given in the SI.) Distances are given in Å. Atoms optimized with 6-31++G(d,p) are represented by balls and those with STO-3G are shown by network in both Figure 1 and Figure 3.

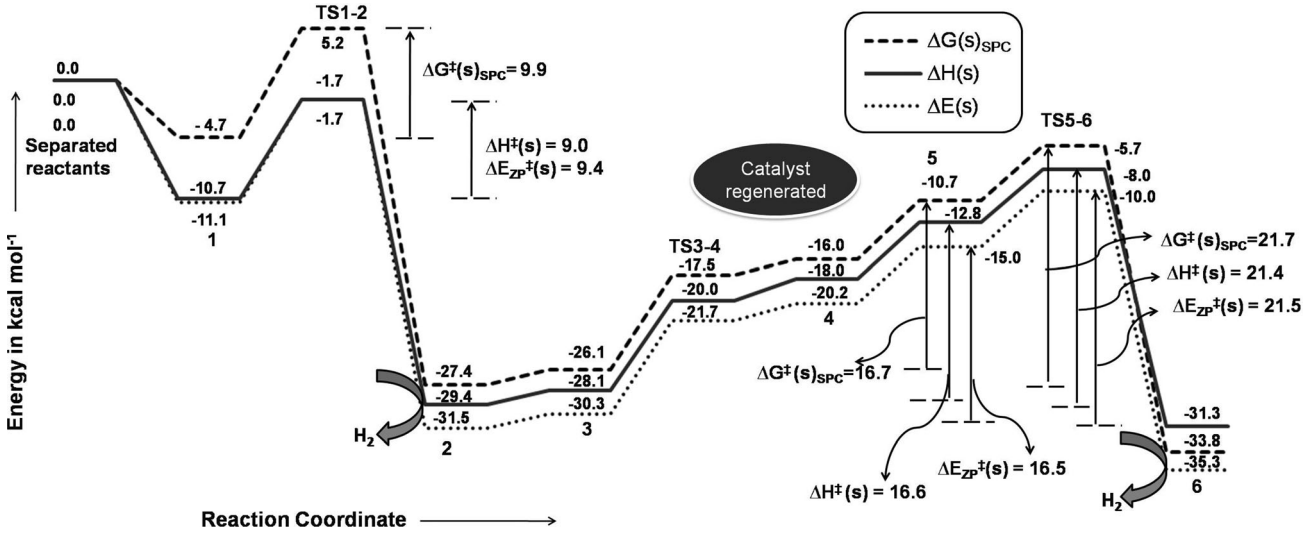

Figure 2. Solvent-phase energy profile diagram of dehydrogenation of 50% hydrogenated (8.0) zigzag BN nanotube of approximately 1 nm length (1-HBNNT) with triflic acid. $\Delta G(s)_{SPC}$, $\Delta H(s)$, and $\Delta E(s)$ are shown by dashed, solid, and dotted lines, respectively.

Table 1: Comparative study of the solvent-phase-corrected Gibbs free energy activation barrier [computed with S(s) = 0.5S(g)] for the dehydrogenation of 1-HBNNT and 2-HBNNT with triflic acid in different DFT functionals. The general trend followed is B3LYP > M05-2X > M06-2X ≈ ωB97XD.

	ωB97XD	M05-2X	M06-2X	B3LYP
TS1-2	9.9	9.0	8.6	15.0
TS3-4	16.7	18.4	16.5	18.7
TS5-6	21.7	22.7	22.0	22.5
TS1′-2′	8.5	7.8	7.5	15.0
TS3′-4′	19.7	21.5	20.0	20.5
TS5′-6′	24.1	25.0	24.7	23.8
TS5′-6′[a]	22.4*	23.0*	22.9*	20.6*

[a] Intermediates and transition states optimized with B3LYP/B1″[18] *Gibbs free energy barriers computed with single-point solvent-phase calculations with the respective functionals and B3 basis set[18] on the B3LYP/B1″-optimized geometries.

molecule from 2-HBNNT **(TS1′-2′)** are slightly lower. The solvent-phase-corrected Gibbs free energy of activation $\Delta G^{\ddagger}(s)_{SPC}$ for both, 1-HBNNT (9.9 kcal mol^{-1}, Figure 2) and 2-HBNNT (8.5 kcal mol^{-1}), are also comparable (see Table 1). A similar transition state was identified for the H_2 release from an analogous chemisorbed hydrogenated (8,0) 1 nm long carbon nanotube and was predicted at an activation energy of 43 kcal mol^{-1} in the gas phase and approximately 40 kcal mol^{-1} in the solvent phase, which is prohibitively high. This result is consistent with the strong C–H bonds in carbon nanotubes (CNTs) reminiscent of the alkane C–H bonds, whereas the B–H and N–H bonds are relatively vulnerable due to their dipolar nature. The higher kinetic barrier in dehydrogenating CNT is due to the difficulty of C–H activation under moderate conditions. The H_2 release from a hydrogenated BN nanotube leads to the formation of an intermediate **2** (Figure 3) comprising hydrogen-bonds between the triflate anion and protons (hydrogens on N–H moieties) of the hydrogenated nanotube surface. The first dehydrogenation is a significantly exothermic process.

Removal of one H_2 formed from the proton of TfOH and the hydride of one of the B–H moieties essentially leaves behind a positively charged HBNNT species hydrogen-bonded to a triflate anion. Unlike the dehydrogenation of AB with TfOH, in the present case we find that the triflate anion forms a very weak bond to an unsaturated B atom at the nanotube surface through one of the O atoms . The B–O interatomic distance is predicted to be 2.52 Å (see Figure 3), which is much longer than the usual B–O bond (1.54 Å). The weak interaction between the surface B atom and O of the triflate does not prove to be a significant hurdle in the regeneration of the catalyst triflic acid. The dehydrogenation cycle can only become catalytic if a proton is abstracted from the positively charged HBNNT species by the triflate anion to regenerate TfOH, which can trigger further dehydrogenations. The triflate anion indeed can abstract a vicinal N–H proton to which it is hydrogen-bonded (**3**, see Figure 3). The overall barrier for acid regeneration turns out to be 16.7 kcal mol^{-1} and the reaction is endergonic as well as endothermic (see Figure 2). The regeneration of the acid indicates that the catalyst is revived after a stoichiometric release of H_2. The

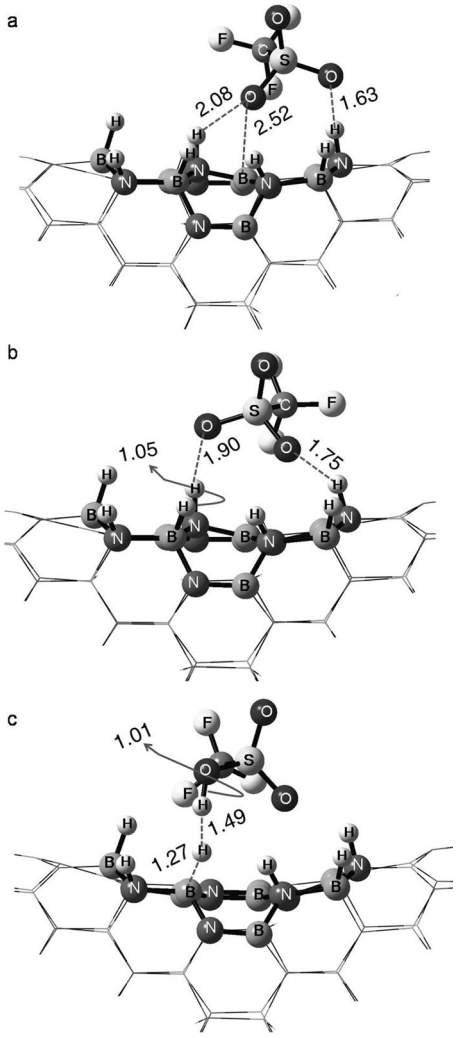

Figure 3. Partial view of the optimized geometry of some of the crucial intermediates during the dehydrogenation of 1-HBNNT with triflic acid: a) 2, b) 3 and c) 5. Full optimized geometries are given in the SI. Distances are given in Å.

sustainability of the catalytic process can only be ensured if the regenerated TfOH can cause another dehydrogenation at a reasonably low barrier. Certainly there are several instances of organic reactions, in which triflic acid has been involved as an active catalytic species.[26] This is in agreement with our mechanistic study. Additionally, reactions involving AB have been studied in acetonitrile solvent[27] suggesting that the choice of solvent for its higher chemical analogue, HBNNT, has been reasonable. The reformation of TfOH would induce further hydrogen loss by protonation of a neighboring B–H bond in a similar pattern (**5**, Figure 3). Analogous to the optimized geometry of **TS1-2**, the hydride (B–H)-proton (O–H) distance is 0.95 Å in **TS5-6** (Figure 1). The removal of a second H_2 molecule from the BN nanotube happens to be the rate-determining step, which occurs at a Gibbs free energy barrier of 5.0 kcal mol^{-1} with regard to intermediate **5**. However, the rate-limiting barrier turns out to be 21.7 and 24.1 kcal mol^{-1} in the solvent phase for 1-HBNNT and 2-HBNNT, respectively. Nevertheless, dislodging the second

molecule of hydrogen by TfOH in acetonitrile solvent from the chosen hexagon at the middle of both the 1 nm long and 2 nm long hydrogenated BN nanotubes at reasonably low barriers is expected to occur at slightly elevated temperatures (40–50 °C). These transition states are followed by intermediates, in which the in situ-formed triflate anion is hydrogen-bonded to several N–H protons of the BN nanotube.

To exclude any discrepancy due to the employment of minimal basis sets for the larger part of the nanotube, the geometries were further optimized at the B3LYP level with higher split-valence basis sets with polarization functions in all parts of the nanotube and the acid catalyst. Single-point solvent-phase and gas-phase energies were refined with the employment of the ωB97XD and dispersion-corrected B3LYP-D method.[18] It was observed that the change of the activation barrier due to the change of the basis set during optimization is in an acceptable range ($\approx$1 to 2 kcal mol^{-1} difference) to ascertain the reliability of the method and the basis sets used in our studies. Furthermore, the predicted rate-determining barrier of 22.4 kcal mol^{-1} with better basis-optimized **TS5′-6′** and the relevant intermediates suggests that the whole reaction would be completed at a significantly faster rate ($\approx 5\times10^{-3}$ s^{-1}) within minutes at mildly elevated temperature (50 °C).[18] Hence, our computational observation suggests that even at room temperature one may expect significant dehydrogenation rates by similar organic acids. Needless to say that such kinetic barrier to dehydrogenation may be further reduced by devising the use of more suitable acids, which will be addressed in future reports.

However, one may suspect that as the percentage coverage would gradually decrease after the dehydrogenation of some of the chemisorbed hydrogens from the HBNNT surface, the subsequent release of H_2 may become difficult. Contrary to this apprehension we find that a 25 %-hydrogenated 1 nm long (8,0) BN nanotube with the triflic acid catalyst shows similar dehydrogenation kinetics. For a 25 %-hydrogenated BNNT the initial hydride–proton coupling is kinetically and thermodynamically favored with a free energy of activation of $\Delta G^{\ddagger}(s)_{SPC} = 6.1$ kcal mol^{-1}, followed by an intermediate, in which a triflate anion is hydrogen-bonded to the protic hydrogens (N–H) of the chemisorbed hydrogenated BNNT. The hydrogen release mechanism after regeneration of the acid also shows a similar trend. The removal of a second equivalent of hydrogen from a ring chosen in the middle of a 25 %-hydrogenated BNNT has a kinetic barrier of $\Delta G^{\ddagger}(s)_{SPC} = 21.8$ kcal mol^{-1}. These comparable results of dehydrogenation from a 1 nm long BNNT having 50 % as well as 25 % chemisorbed hydrogen coverage shows that the acid catalyst could remove chemisorbed hydrogens from both the nanotubes with equal ease. Even with lower hydrogen coverage we find the predicted barriers for such a type of dehydrogenation are similar to the aforementioned cases.[18] Hence the removal of hydrogens would be completed at moderate conditions (40–50 °C) in the presence of the catalyst, whereas the noncatalytic route by thermal dehydrogenation takes place at very high temperatures ($\approx$400 °C). This finding surely prompts toward a feasible dehydrogenation strategy of chemisorbed hydrogens from a hydrogenated BN nanotube by simple organic acid molecules.

In conclusion we state that we have unravelled a hydrogen release strategy from chemically hydrogenated BN nanotubes with the aid of a strong Brønsted acid, triflic acid. Our computational study reveals that H_2 can be released from BN nanotube surfaces bearing chemisorbed hydrogen at low kinetic barriers using a "metal-free" reagent. The onset of thermal dehydrogenation in hydrogenated BNNTs in the absence of a catalyst is initiated at a very high temperature (above 350 °C). The remarkable aspect of the acid-catalyzed dehydrogenation is that such a feat can possibly be attained at much lower temperatures, which are rather close to room temperature. The outlined chemistry significantly enhances the prospect of developing a chemical hydrogen storage strategy based on boron nitride nanomaterials.

Received: March 23, 2014
Revised: June 27, 2014
Published online: August 11, 2014

Keywords: Brønsted acid · dehydrogenation · density functional calculations · main group elements · nanotubes

[1] a) The Hydrogen Economy: NRC and NAE, The National Academic press, Washington, DC, **2004**; b) Targets for Onboard Hydrogen Storage Systems for Light-Duty Vehicles, U.S. DOE, September **2009**. http://energy.gov/sites/prod/files/2014/03/f11/targets_onboard_hydro_storage_explanation.pdf.

[2] a) T. Yildirim, M. R. Hartman, *Phys. Rev. Lett.* **2005**, *95*, 215504; b) H. Lee, J.-w. Lee, D. Y. Kim, J. Park, Y.-T. Seo, H. Zeng, I. L. Moudrakovski, C. I. Ratcliffe, J. A. Ripmeester, *Nature* **2005**, *434*, 743–746; c) A. C. Dillon, K. M. Jones, T. A. Bekkedahl, C. H. Kiang, D. S. Bethune, M. J. Heben, *Nature* **1997**, *386*, 377–379; d) Y. Zhao, Y.-H. Kim, A. C. Dillon, M. J. Heben, S. B. Zhang, *Phys. Rev. Lett.* **2005**, *94*, 155504; e) B. Bogdanović, M. Felderhoff, S. Kaskel, A. Pommerin, K. Schlichte, F. Schüth, *Adv. Mater.* **2003**, *15*, 1012–1015; f) Z. Xiong, C. K. Yong, G. Wu, P. Chen, W. Shaw, A. Karkamkar, T. Autrey, M. O. Jones, S. R. Johnson, P. P. Edwards, W. I. F. David, *Nat. Mater.* **2008**, *7*, 138–141.

[3] a) T. B. Marder, *Angew. Chem. Int. Ed.* **2007**, *46*, 8116–8118; *Angew. Chem.* **2007**, *119*, 8262–8264; b) C. W. Hamilton, R. T. Baker, A. Staubitz, I. Manners, *Chem. Soc. Rev.* **2009**, *38*, 279–293; c) A. Staubitz, A. P. M. Robertson, I. Manners, *Chem. Rev.* **2010**, *110*, 4079–4124; d) G. Alcaraz, S. Sabo-Etienne, *Angew. Chem. Int. Ed.* **2010**, *49*, 7170–7179; *Angew. Chem.* **2010**, *122*, 7326–7335.

[4] a) A. D. Sutton, A. K. Burrell, D. A. Dixon, E. B. Garner III, J. C. Gordon, T. Nakagawa, K. C. Ott, J. P. Robinson, M. Vasiliu, *Science* **2011**, *331*, 1426–1429; b) G. R. Whittell, I. Manners, *Angew. Chem. Int. Ed.* **2011**, *50*, 10288–10289; *Angew. Chem.* **2011**, *123*, 10470–10472.

[5] B. E. Smith, R. L. Richards, W. E. Newton, *Catalysts for Nitrogen fixation*, Springer, Dordrecht, **2004**.

[6] R. Ma, Y. Bando, H. Zhu, T. Sato, C. Xu, D. Wu, *J. Am. Chem. Soc.* **2002**, *124*, 7672–7673.

[7] C. Tang, Y. Bando, X. Ding, S. Qi, D. Golberg, *J. Am. Chem. Soc.* **2002**, *124*, 14550–14551.

[8] S. H. Lim, J. Luo, W. Ji, J. Lin, *Catal. Today* **2007**, *120*, 346–350.

[9] a) D. Golberg, Y. Bando, Y. Huang, T. Terao, M. Mitome, C. Tang, C. Zhi, *ACS Nano* **2010**, *4*, 2979 – 2993; b) D. Golberg, Y. Bando, C. Tang, C. Zhi, *Adv. Mater.* **2007**, *19*, 2413 – 2432.
[10] a) N. G. Chopra, R. J. Luyken, K. Cherrey, V. H. Crespi, M. L. Cohen, S. G. Louie, A. Zettl, *Science* **1995**, *269*, 966 – 967; b) E. Bengu, L. D. Marks, *Phys. Rev. Lett.* **2001**, *86*, 2385 – 2387.
[11] a) X. Wu, J. Yang, J. G. Hou, Q. Zhu, *J. Chem. Phys.* **2004**, *121*, 8481 – 8485; b) S. S. Han, S. H. Lee, J. K. Kang, H. M. Lee, *Phys. Rev. B* **2005**, *72*, 113402.
[12] X. Chen, X. P. Gao, H. Zhang, Z. Zhou, W. K. Hu, G. L. Pan, H. Y. Zhu, T. Y. Yan, D. Y. Song, *J. Phys. Chem. B* **2005**, *109*, 11525 – 11529.
[13] a) A. Nikitin, H. Ogasawara, D. Mann, R. Denecke, Z. Zhang, H. Dai, K. Cho, A. Nilsson, *Phys. Rev. Lett.* **2005**, *95*, 225507; b) D. C. Elias, R. R. Nair, T. M. G. Mohiuddin, S. V. Morozov, P. Blake, M. P. Halsall, A. C. Ferrari, D. W. Boukhvalov, M. I. Katsnelson, A. K. Geim, K. S. Novoselov, *Science* **2009**, *323*, 610 – 613.
[14] K. S. Subrahmanyam, P. Kumar, U. Maitra, A. Govindaraj, K. P. S. S. Hembram, U. V. Waghmare, C. N. R. Rao, *Proc. Natl. Acad. Sci. USA* **2011**, *108*, 2674 – 2677.
[15] L. Roy, S. Mittal, A. Paul, *Angew. Chem. Int. Ed.* **2012**, *51*, 4152 – 4156; *Angew. Chem.* **2012**, *124*, 4228 – 4232.
[16] P. M. Zimmerman, Z. Zhang, C. B. Musgrave, *Inorg. Chem.* **2010**, *49*, 8724 – 8728.
[17] For recent reports on ammonia borane dehydrocoupling by transition-metal-based catalysts, see: a) A. Paul, C. B. Musgrave, *Angew. Chem. Int. Ed.* **2007**, *46*, 8153 – 8156; *Angew. Chem.* **2007**, *119*, 8301 – 8304; b) P. M. Zimmerman, A. Paul, Z. Zhang, C. B. Musgrave, *Angew. Chem. Int. Ed.* **2009**, *48*, 2201 – 2205; *Angew. Chem.* **2009**, *121*, 2235 – 2239; c) H. Helten, B. Dutta, J. R. Vance, M. E. Sloan, M. F. Haddow, S. Sproules, D. Collison, G. R. Whittell, G. C. Lloyd-Jones, I. Manners, *Angew. Chem. Int. Ed.* **2013**, *52*, 437 – 440; *Angew. Chem.* **2013**, *125*, 455 – 458; d) R. T. Baker, J. C. Gordon, C. W. Hamilton, N. J. Henson, P.-H. Lin, S. Maguire, M. Murugesu, B. L. Scott, N. C. Smythe, *J. Am. Chem. Soc.* **2012**, *134*, 5598 – 5609; e) B. L. Conley, D. Guess, T. J. Williams, *J. Am. Chem. Soc.* **2011**, *133*, 14212 – 14215; f) B. L. Conley, T. J. Williams, *Chem. Commun.* **2010**, *46*, 4815 – 4817.
[18] See the Supporting Information for details.
[19] a) J.-M. Denis, H. Forintos, H. Szelke, L. Toupet, T.-N. Pham, P.-J. Madec, A.-C. Gaumont, *Chem. Commun.* **2003**, 54 – 55; b) F. H. Stephens, R. T. Baker, M. H. Matus, D. J. Grant, D. A. Dixon, *Angew. Chem. Int. Ed.* **2007**, *46*, 746 – 749; *Angew. Chem.* **2007**, *119*, 760 – 763.
[20] S. Bhunya, A. Banerjee, R. Tripathi, N. N. Nair, A. Paul, *Chem. Eur. J.* **2013**, *19*, 17673 – 17678.
[21] a) A. D. Becke, *J. Chem. Phys.* **1993**, *98*, 5648 – 5652; b) J.-D. Chai, M. Head-Gordon, *Phys. Chem. Chem. Phys.* **2008**, *10*, 6615 – 6620; c) Y. Zhao, N. E. Schultz, D. G. Truhlar, *J. Chem. Theory Comput.* **2006**, *2*, 364 – 382; d) Y. Zhao, D. G. Truhlar, *Theor. Chem. Acc.* **2008**, *120*, 215 – 241.
[22] a) "Entropies of Condensed Phases and Complex Systems": C. Spickermann, Springer Theses, **2010**, Chap. 3, pp. 76 – 80, and references therein; b) D. H. Wertz, *J. Am. Chem. Soc.* **1980**, *102*, 5316 – 5322; c) H. Li, X. Wang, F. Huang, G. Lu, J. Jiang, Z.-X. Wang, *Organometallics* **2011**, *30*, 5233 – 5247.
[23] a) V. Barone, M. Cossi, *J. Phys. Chem. A* **1998**, *102*, 1995 – 2001; b) M. Cossi, N. Rega, G. Scalmani, V. Barone, *J. Comput. Chem.* **2003**, *24*, 669 – 681.
[24] V. M. Sánchez, M. Sued, D. A. Scherlis, *J. Chem. Phys.* **2009**, *131*, 174108.
[25] R. Buzzoni, S. Bordiga, G. Ricchiardi, G. Spoto, A. Zecchina, *J. Phys. Chem.* **1995**, *99*, 11937 – 11951.
[26] a) D. C. Rosenfeld, S. Shekhar, A. Takemiya, M. Utsunomiya, J. F. Hartwig, *Org. Lett.* **2006**, *8*, 4179 – 4182; b) Z. Li, J. Zhang, C. Brouwer, C.-G. Yang, N. W. Reich, C. He, *Org. Lett.* **2006**, *8*, 4175 – 4178, and references therein.
[27] J. S. Wang, R. A. Geanangel, *Inorg. Chim. Acta* **1988**, *148*, 185 – 190.

